

Evaluation of the Physicochemical and Antioxidative Properties of Curcumin Metallocomplexes in Self-Microemulsifying Drug Delivery Systems

Wei Sean Mah¹   Shu Xian and Chong^{*,1}  

¹Faculty of Pharmacy, SEGi University, Selangor, Malaysia.

*Corresponding author

Received 26/4/2024, Accepted 10 /9/2024, Published 20/12/2025



This work is licensed under a Creative Commons Attribution 4.0 International License.

Abstract

Curcumin (CUR), an active constituent of turmeric which is capable of forming complexes with metal ions. Even though CUR metallocomplexes displayed better biological activities compared to the free CUR, their application in medicine is limited by their poor aqueous solubility. This research aimed to develop self-microemulsifying drug delivery systems (SMEDDSs) to improve the solubility and the antioxidative activity of CUR metallocomplexes. Mononuclear (1:1) CUR metallocomplexes (CUR-Cu, CUR-Mg and CUR-Fe) were synthesized with Cu^{2+} , Mg^{2+} and Fe^{3+} salts. The CUR and CUR metallocomplexes were loaded into the microemulsions (MEs) which contains palm oil, Tween 80 and polyethylene glycol (PEG) 400 at the ratios of 1:7:2 and 1:8:1. All of the MEs formulations appeared to be monophasic and clear, where the pH values were in the range of 6.55-6.78. In both formulations, the solubility of all metallocomplexes were 1.3-3.4-folds higher than the CUR, where CUR-Cu MEs (1:7:2 and 1:8:1) exhibited the highest solubility ($965.99 \pm 102.59 \mu\text{g/mL}$ and $986.49 \pm 75.31 \mu\text{g/mL}$, respectively). In both formulations, CUR-Cu MEs displayed ~2-folds higher %RSA compared to CUR MEs, meanwhile; CUR-Fe displayed the lowest %RSA (~6-7%) which may be due to the instability of the coordination of ligand-metal complex resulted from the high oxidation state in Fe^{3+} ion.

Keywords: Antioxidative Properties, Curcumin, Physicochemical Properties, Metallocomplexes, SMEDDS.

Introduction

CUR presents as a diketone tautomer and a keto-enol tautomer (Figure. 1), where the latter form is the most stable form ⁽¹⁾. The diketone group of CUR undergoes keto-enol tautomerism, which allows CUR to chelate many metal ions ⁽²⁾. Studies showed that formation of CUR metallocomplexes destabilized the diketo ($\text{C}=\text{O}$) bond strengths due to the charge transfer from the oxygen atoms to the metal ions ⁽²⁾. The instability of CUR in biological media is closely associated with the presence of the diketo site of CUR undergoing tautomeric equilibrium ⁽³⁾. The formation of metallocomplexes causes the tautomeric equilibrium to shift toward the keto-enol form, increasing the in vitro stability of CUR at physiological pH ⁽³⁾. CUR forms stable metallocomplexes with 1:1 and 1:2 metal: ligand chelating modes by reaction between CUR with divalent or trivalent metal ions (Figure. 2). Also, the antioxidant activity of the 1:1 CUR- Cu^{2+} complex was found to be superior compared to the 1:2 metal complex because it demonstrates a significant tetrahedral distortion from square planar geometry when reacted with the superoxide radicals. This enables the 1:1 CUR- Cu^{2+} complex to remain integral and go through multiple redox cycles. In

contrast, the planar but rigid structure in 1:2 CUR- Cu^{2+} complex (Figure. 2) makes it a less potent antioxidant due to its inability to undergo distortions ⁽⁴⁾. A series of complexes of CUR with Mg^{2+} , Mn^{2+} , Fe^{2+} , Cu^{2+} , B^{2+} , Se^{2+} and Zn^{2+} ions have been synthesized to study their antioxidant activity by 2,2-diphenyl-1-picrylhydrazyl (DPPH) radical scavenging assay. The study revealed that CUR-Zn complex imparted the strongest antioxidant activity ($\text{IC}_{50} = 0.41 \text{ mM}$) compared to free CUR ($\text{IC}_{50} = 1.15 \text{ mM}$) ⁽⁵⁾. Another in vitro study also demonstrated that the antioxidant activity of CUR-Cu was 3-folds higher than the free CUR and displayed a comparable activity to butylated hydroxytoluene ⁽⁶⁾. The antioxidative activity of CUR is greatly contributed by the presence of methoxylated phenols in the structure of CUR. The acetylated CUR metallocomplexes at the hydroxyl ($-\text{OH}$) of the aromatic rings of CUR resulted in reduced in antioxidant capacity compared to CUR metallocomplexes with free phenolic OH the aromatic rings ⁽⁷⁾. The objectives of this study are to synthesize mononuclear 1:1 CUR metallocomplexes by complexation of CUR with metal ions (Cu^{2+} , Mg^{2+} and Fe^{3+}) and load the CUR and CUR

metallocomplexes into SMEDDSs. By this end, the solubility and antioxidative activity of CUR and

CUR metallocomplexes in SMEDDSs were evaluated.

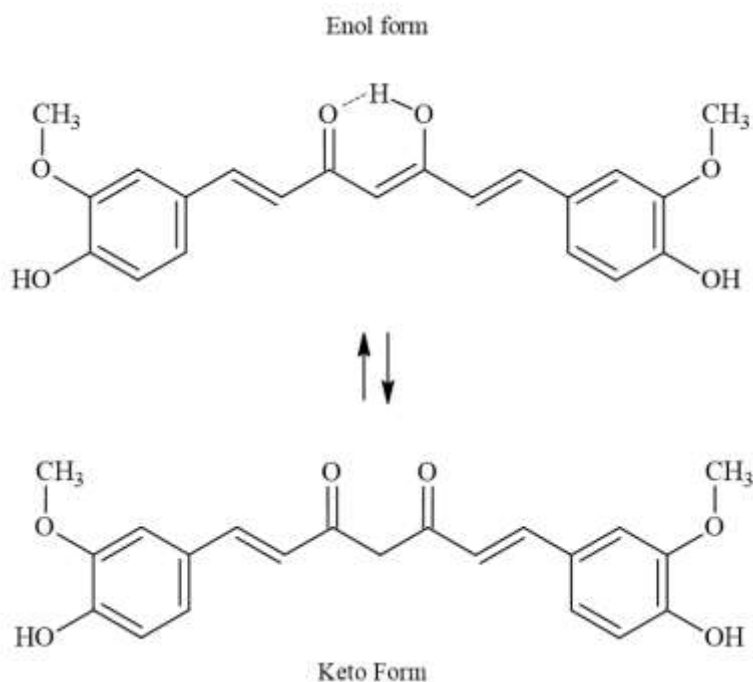


Figure 1. Tautomerism of CUR into keto-enol form

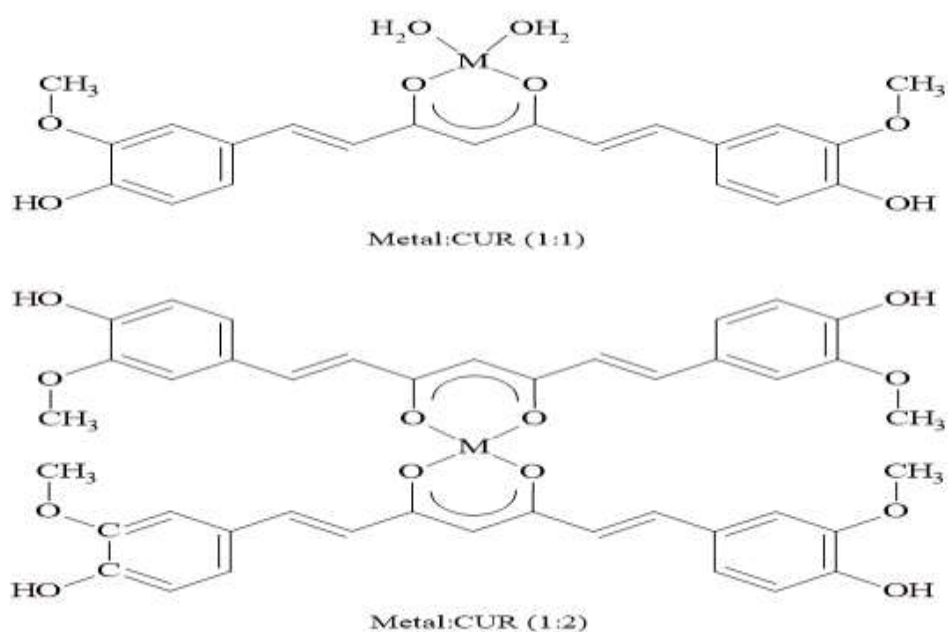


Figure 2. Chemical structures of mononuclear (1:1) and binuclear (1:2) metal:CUR complexes

SMEDDS has been developed as an alternative oral formulation to circumvent the problems of poor aqueous solubility and oral absorption of hydrophobic compounds, such as celecoxib⁽⁸⁾, simvastatin⁽⁹⁾, and ferulic acid⁽¹⁰⁾. It is a thermodynamically stable nanocarrier with an

isotropic combination of oil, surfactant and co-surfactant which spontaneously forms a self-assembling oil-in-water (O/W) ME when diluted with gastrointestinal tract fluids⁽¹¹⁾. Studies have shown that the incorporation of a drug into SMEDDS improves drugs' distribution into the

brain, liver, lung and spleen ^(10,12,13). SMEDDS provides long-term physical and/or chemical stability due to the absence of water content outside the body ⁽¹⁴⁾. SMEDDS is a lipid-based nanocarrier known for its solubility, stability, improved absorption and facilitated bioavailability. It may be an effective carrier system to improve the pharmacokinetic profile of CUR metallocomplexes.

Materials and Methods

Materials

CUR (95%) and 2,2-diphenyl-1-picrylhydrazyl (DPPH) were procured from Alfa Aesar, United Kingdom. Copper (II) sulphate pentahydrate ($\text{CuSO}_4 \cdot 5\text{H}_2\text{O}$), magnesium sulphate heptahydrate ($\text{MgSO}_4 \cdot 7\text{H}_2\text{O}$) and Tween 80 were procured from Systerm, Malaysia. Iron (III) chloride anhydrous (FeCl_3) and methanol were procured from Chemiz, Malaysia). PEG 400 and palm oil were procured from ChemSoln, Malaysia and Bendosen Laboratory Chemicals, Norway, respectively.

Synthesis and characterization of CUR metallocomplexes

A mononuclear (1:1) CUR-Cu complex was prepared by dissolving 1 mol of CUR and 1 mol of $\text{CuSO}_4 \cdot 5\text{H}_2\text{O}$ in 70% methanol and stirred for 2 hours at 40°C. The precipitate was vacuum filtered, washed with cold water and dried overnight in an oven at 40°C ⁽¹⁵⁾. The procedures were similar for the synthesis of CUR-Mg and CUR-Fe complexes. All of the metallocomplexes were characterized by

Table 1. Composition of SMEDDS formulations for CUR and CUR metallocomplexes.

Formulation	Weight Ratio		
	Palm oil	Tween 80	PEG 400
SMEDDS (1:7:2)	1	7	2
SMEDDS (1:8:1)	1	8	1

pH of CUR metallocomplexes in SMEDDSs

The pH of all SMEDDSs were determined by pH meter (Eutech Instruments CyberScan pH/mV/°C meter pH 510). All measurements were done in triplicates.

Concentration of CUR metallocomplexes in SMEDDSs

The concentrations of CUR and CUR metallocomplexes presence in SMEDDSs (1:7:2 and 1:8:1) were determined from the calibration curve of CUR and CUR metallocomplexes. The samples were diluted with methanol within the linear range of the calibration curve (1.25, 2.5, 5, 10 and 20 $\mu\text{g/mL}$) and their absorbances were measured at 420 nm using ultraviolet-visible (UV-vis) spectrophotometer (Shimadzu UVmini-1240, Japan).

Nevertheless, there is a lack of literature on the physicochemical and antioxidative properties of CUR metallocomplexes in SMEDDSs. In this study, the pH, solubility and antioxidative properties of CUR metallocomplexes (CUR-Cu, CUR-Mg and CUR-Fe) were compared to the metallocomplexes in SMEDDS formulations.

Fourier Transform Infrared (FTIR) spectrometer (PerkinElmer Spectrum 100, US) where the spectra were scanned on the wave number range of 4000-650 cm^{-1} . The λ_{max} of CUR and CUR metallocomplexes in methanol were determined by UV-Vis spectrophotometer (Shimadzu UVmini-1240) with the wavelength range of 300-650 nm.

Preparation of CUR metallocomplexes in SMEDDSs

CUR in SMEDDSs were prepared as described by Muniandy and Chong ⁽¹⁶⁾. 10 mg CUR was loaded into 1 mL palm oil and stirred overnight. The mixture was filtered through a 0.45 μm millipore membrane filter. The palm oil containing CUR was added to Tween 80 and PEG 400 at different ratios (Table 1), with a total volume of 10 mL and stirred overnight ⁽¹⁶⁾. The procedures were similar for the preparation of CUR metallocomplexes in MEs. All of the CUR SMEDDSs were characterised by FTIR spectroscopy which shows the presence of encapsulated compound in SMEDDSs by analyzing the functional groups.

Solubility of CUR and CUR metallocomplexes in water and SMEDDSs

Excess CUR and its metallocomplexes were added to 2 mL of distilled water to ensure the solution is saturated. The mixtures are agitated overnight and centrifugated at a speed of 14,000 rpm for 10 minutes. The mixtures were filtered to collect the residue. The residue is then diluted with methanol within the linear range of the calibration curve using UV-Vis spectrophotometer at 420 nm (Shimadzu UVmini-1240, Japan). The procedures were repeated for the study of the solubility of CUR and its metallocomplexes in SMEDDSs (1:7:2 and 1:8:1) where excess CUR and its metallocomplexes were added to 2 mL of SMEDDSs.

Antioxidative activity of CUR and CUR metallocomplexes in SMEDDS

0.2 mM DPPH solution was freshly prepared with methanol. 1 mg/mL solutions of CUR, CUR-Cu, CUR-Mg and CUR-Fe were dissolved in methanol, and 50 μ L of each of these solutions was added to 2950 μ L of DPPH solution. The DPPH solution was served as a blank. The mixtures were shaken and incubated for 15 minutes in the dark. The absorbance was quantified spectrophotometrically at 517 nm against the DPPH solution⁽¹⁷⁾. The procedures were repeated for SMEDDS where 50 μ L of CUR, CUR-Cu, CUR-Mg and CUR-Fe SMEDDSs were added to 2950 μ L of DPPH solution for analysis. The % radical scavenging activity (RSA) was calculated using the following equation:

$$\%RSA = \frac{(\text{Absorbance of the blank} - \text{Absorbance of sample})}{\text{Absorbance of the blank}} \times 100$$

Statistical analysis





The statistical analysis was conducted using a two-tailed t-test to determine the difference between the two groups' means, where $p < 0.05$ was regarded as statistically significant. All data were analyzed using Microsoft Excel (Microsoft Office Professional Plus 2019, Washington, United States).

Results and Discussion

Synthesis and characterization of curcumin metallocomplexes

CUR and the metals should be dissolved in a solution in order for the chemical reaction to take place⁽¹⁸⁾. In this study, 70% methanol were used to dissolve the metal salts and CUR which is poorly soluble in water. The reactants are readily dissolved in methanol as methanol has a middling polarity index of 5.1⁽¹⁹⁾. In the methanolic solution, the predominant form of CUR exists as the keto-enol tautomeric form⁽²⁰⁾. The -OH group in the keto-enol site of CUR is deprotonated, leading to the formation of a β -diketonate which coordinates to an ion in a bidentate fashion (Figure. 2)⁽²¹⁾. The stability of metallocomplexes is also modulated by the electronic and steric factors in the chemical structure of CUR, wherein the latter factor can prevail. The three oxygen atoms in CUR potentially act as an electron donor to interact with the metals. However, the steric repulsion between ortho-oxygen atoms in the phenyl ring reduces the binding of metals to these positions, thus, it is the oxygen atoms in the C=O is a site of interaction to the metals⁽²²⁾. Three CUR metallocomplexes of Cu^{2+} , Mg^{2+} and Fe^{3+} appeared as powders with distinct colours. The % of yield for all of the CUR metallocomplexes were $>80\%$ (Table 2).

Table 2. Percent yield and physical appearance of CUR and CUR metallocomplexes.

Compound	% yield	Physical appearance	
CUR	-	Orange-yellow powder	
CUR-Cu	99.81	Brown powder	
CUR-Mg	86.67	Bright yellow powder	
CUR-Fe	81.04	Black powder	

The FTIR spectrum of CUR and CUR metallocomplexes are shown in Figure. 3. The stretching vibration of C=O moiety in CUR, CUR-Mg, CUR-Cu and CUR-Fe complexes were detected at 1626, 1627, 1625 and 1621 cm^{-1} , respectively. A slight decline in the intensity of the C=O band implies that the C=O groups were involved in the conjugation with the metal ions⁽²³⁾. The vibrational stretches of C=C were expressed at 1509 cm^{-1} . The peaks detected at 1429 cm^{-1} and 1282 cm^{-1} indicated

vibrational bending of C-H groups and stretching vibrations of aromatic C-O groups, respectively. Stretching of the -OCH₃ groups was observed at 1026 cm^{-1} ^(22,24). Moreover, the aromatic C-O stretching vibrations were shifted from 1282.39 cm^{-1} to 1281.37, 1282.21 and 1283.36 cm^{-1} for CUR-Cu, CUR-Mg and CUR-Fe, respectively; which indicating the formation of metallocomplexes. The UV-Vis absorption of CUR showed a maximum absorption peak at 420 nm in methanolic solution,

which is consistent with previous reports ^(20,25). The keto-enol tautomer of CUR predominates in the presence of polar organic solvent (methanol) ⁽²⁶⁾ which results in the existence of intramolecular hydrogen bonding in the keto-enol site that makes the π conjugation remain intact within the molecule. The $\pi \rightarrow \pi^*$ electronic transition of the extended conjugation system gives rise to a maximum absorption peak at 420 nm ⁽⁶⁾. The formation of metallocomplexes caused a shift in the maximum

absorption band to a higher wavelength, suggesting that the C=O group of CUR participates in metal chelation. CUR metallocomplexes in methanolic solution exhibited a maximum absorption band at 420 nm and a weak absorption peak at nearly 445 nm (Table 3), corresponding to the strong complexation between CUR and metal ions ⁽²⁴⁾. The two absorption peaks are associated with the charge transfer from the ligand to metals ⁽²⁷⁾.

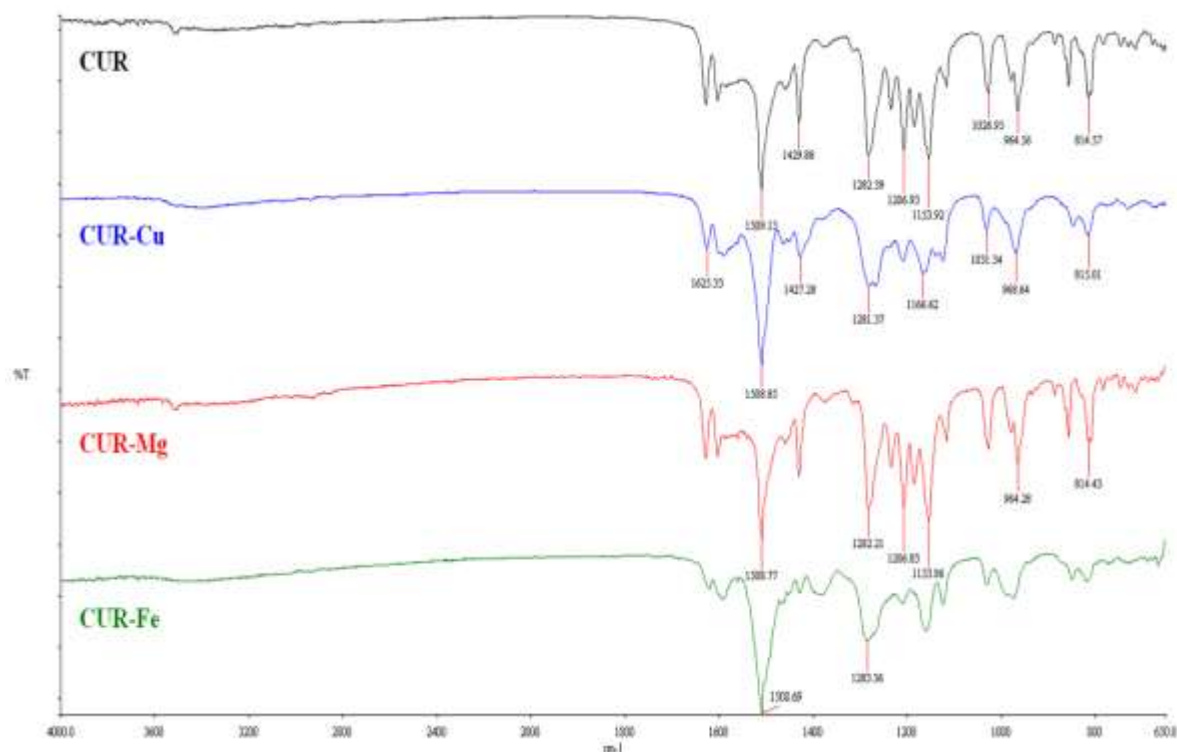


Figure 3. FTIR spectra of CUR and CUR metallocomplexes

Table 3. UV-vis spectra data of CUR and CUR metallocomplexes in methanol.

Compound	UV-Vis peak (nm)	
CUR	420.0	-
CUR-Cu	420.0	~ 445.0
CUR-Mg	420.0	~ 445.0
CUR-Fe	420.0	~ 445.0

Formulation of curcumin metallocomplexes in SMEDDSs

A high surfactant/co-surfactant-to-oil ratio of 9:1 produces thermodynamically stable CUR-containing SMEDDS formulations with high drug solubilization capacity to enhance the shelf-life and physicochemical properties of CUR. In this study ⁽¹⁶⁾, the SMEDDS formulations were composed of palm oil, Tween 80 and PEG 400 as oil, surfactant and co-surfactant, respectively, at ratios of 1:7:2 and 1:8:1. Palm oil is a natural oil which consists of a long triglycerides chain that makes it capable of solubilizing the hydrophobic CUR ⁽²⁸⁾. A SMEDDS employing an oil with long hydrocarbon chains exhibits superior resistance to lipolysis compared to

a SMEDDS with medium-chain triglycerides ⁽¹³⁾. To microemulsify the palm oil, a high amount of surfactant (Tween 80) is used ⁽²⁸⁾ as the unsaturation in the C18 fatty acid chain facilitates the formation of SMEDDS ⁽²⁹⁾. The choice of surfactant and co-surfactant are based on their hydrophilic-lipophilic balance (HLB) values. The water-soluble surfactants (HLB value >12) are usually utilized in formulating a SMEDDS owing to their enhanced micelle-forming capabilities ⁽¹⁴⁾. Meanwhile, surfactants with a HLB value of <10 are essential for reducing the interfacial tension of films between the oil and water phases and increasing the flexibility of the films ⁽¹²⁾. Thus, a combination of surfactants, PEG 400 and Tween 80 with HLB value of 8.5 and

15, respectively; were used to strengthen the stability of the formulation. Self-emulsification can be evaluated through visual assessment. After dilution of samples with water at a 1:10 ratio, the formation of SMEDDS is denoted by the monophasic and clear appearance, while a solution with a cloudy appearance signifies the formation of macroemulsion⁽³⁰⁾. In this study, all SMEDDS formulations appeared as monophasic and transparent liquids at room temperature without signs of physical instability such as phase separation. Visual assessment is also a method of evaluating drug precipitation in a diluted SMEDDS, which commonly happens if a formulation includes a water-soluble co-solvent such as PEG 400⁽³⁰⁾. All SMEDDS formulations were stable as the precipitation of the drug was not evident. No crystal liquid was observed, which could take place due to the high amount of surfactant in SMEDDSs⁽³¹⁾.

Characterization of curcumin metallocomplexes in SMEDDSs

As depicted in the FTIR spectra of PEG 400, palm oil and Tween 80, the absorption peaks at ~ 2900 - 2800 cm^{-1} corresponded to the C-H stretching vibrations of methylene groups. Palm oil and Tween 80 showed peaks at 1746 cm^{-1} and 1735 cm^{-1} , representing the stretching vibration of the C=O group in palm oil and Tween 80 (Figure. 4). The FTIR spectra of CUR and CUR metallocomplexes in SMEDDSs 1:7:2 (Figure. 5) and 1:8:1 (Figure. 6) were similar to one another. All of the SMEDDSs formulations exhibited peaks at ~ 2923 - 2860 cm^{-1} (C-H stretching) and 1738 cm^{-1} (C=O stretching). The characteristic peaks of CUR and CUR metallocomplexes (C=O stretching at $\sim 1626\text{ cm}^{-1}$, C=C stretching at $\sim 1509\text{ cm}^{-1}$, C-H bending at ~ 1429 and $\sim 1282\text{ cm}^{-1}$, and aromatic C-O bending at $\sim 1280\text{ cm}^{-1}$) were absent in all SMEDDSs, corroborating that the compounds were encapsulated in the SMEDDSs due to solubilisation by Tween 80⁽³²⁾.

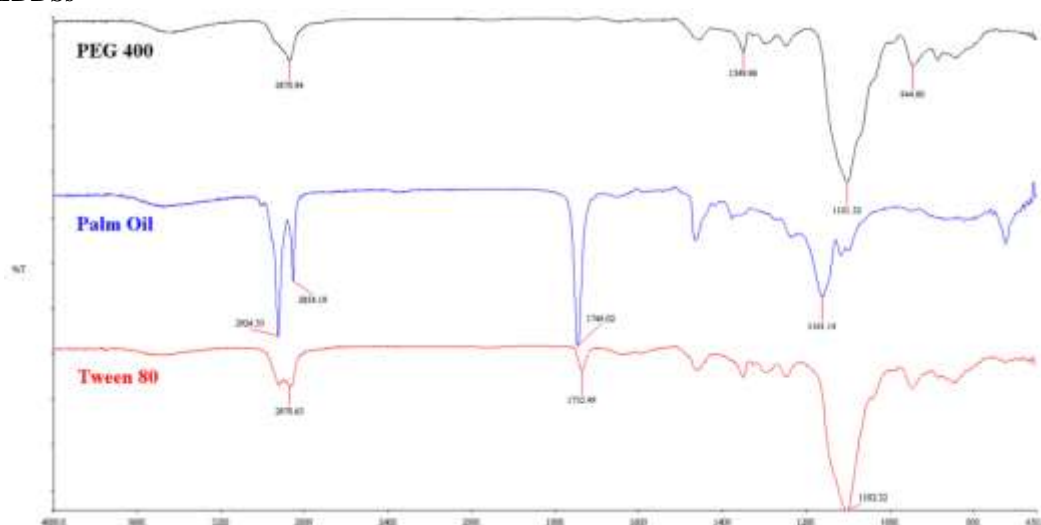


Figure 4. FTIR spectra of PEG 400, palm oil and Tween 80

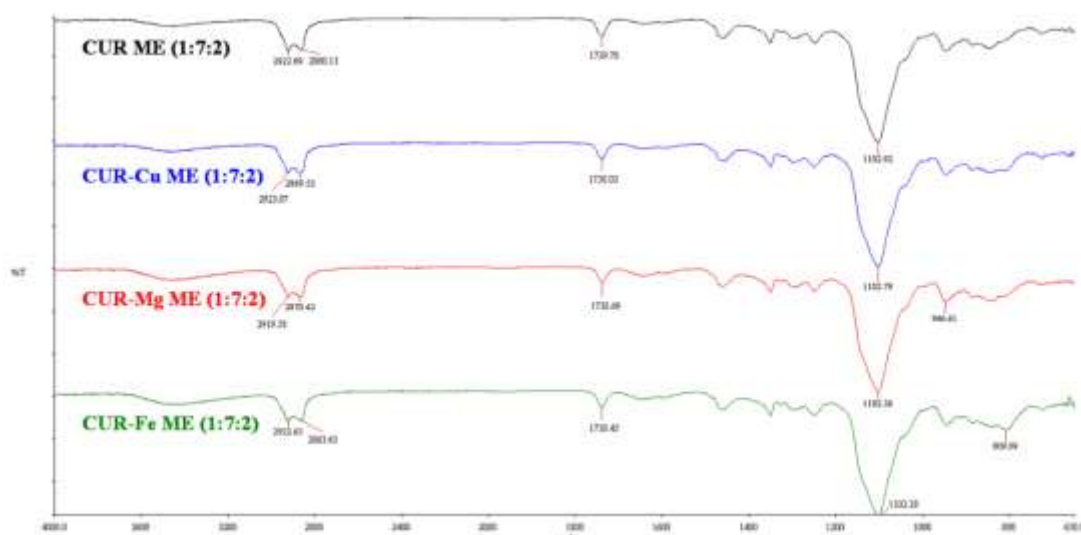


Figure 5. FTIR spectra of CUR and CUR metallocomplexes in SMEDDSs (1:7:2)

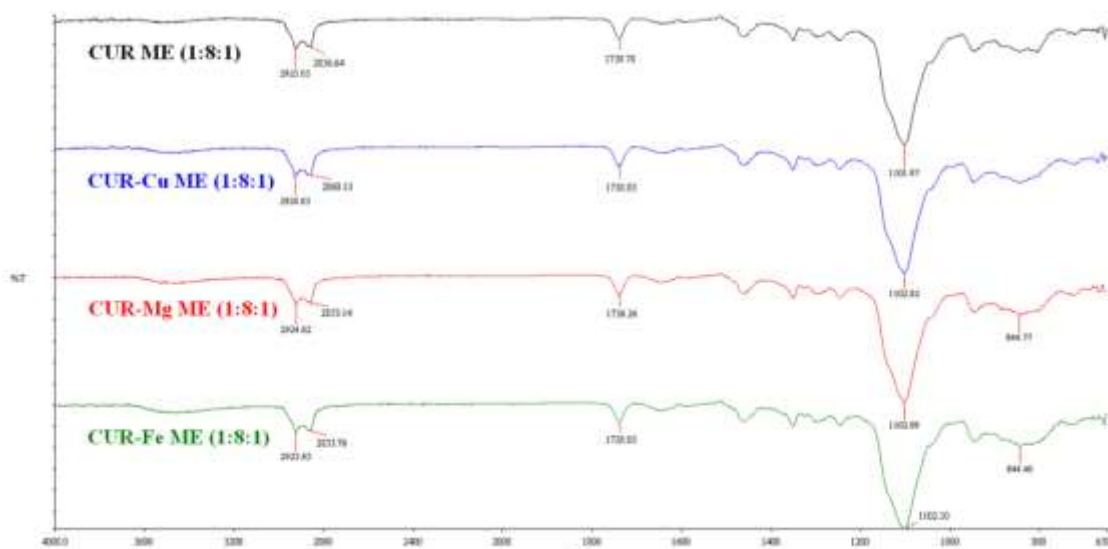


Figure 6. FTIR spectra of CUR and CUR metallocomplexes in SMEDDSs (1:8:1)

pH of CUR metallocomplexes in SMEDDSs

The free CUR was highly unstable under neutral-basic pH (pH > 7.5) conditions and undergoes extensive degradation⁽³³⁾ while CUR metallocomplexes were very stable under pH 6.5-7 compared to free CUR.^(7,35) Both free CUR and its metallocomplexes were unstable under acidic condition (pH 2) but the metallocomplexes were generally more stable compared to free CUR^(5,33). All of the SMEDDSs displayed pH in the range of 6.55 -6.78, which are near to neutral which is ideal for the stability of CUR and CUR metallocomplexes. (Table 4). This indicated that the drug dissolves in the oil and remains in the dispersed phase (oil) and does not disperse into the external phase⁽³⁴⁾.

Concentration of CUR metallocomplexes in SMEDDSs

As shown in Table 4, all of the metallocomplexes displayed higher amount in SMEDDSs than the free CUR. The concentration of metallocomplexes in either SMEDDSs composition decreased in the order of: CUR-Cu > CUR-Fe > CUR-Mg > CUR. In both formulations, CUR-Cu, CUR-Fe and CUR-Mg exerted ~3-, 2.6–3-, and 1.3–1.5-folds, respectively; increase in concentration compared to free CUR. The two-tailed t-test showed significant differences in concentrations between CUR, CUR-Cu and CUR-Fe in both formulations ($p < 0.05$).

Table 4. pH, concentration of CUR or CUR metallocomplexes in SMEDDSs, and folds of increased in concentration of CUR metallocomplexes in SMEDDSs (1:7:2 and 1:8:1).

Formulation		pH	Concentration of CUR or CUR metallocomplexes in SMEDDSs (µg/mL)	Folds of increased in CUR metallocomplexes in SMEDDSs compared to CUR
SMEDDS (1:7:2)	CUR	6.75 ± 0.27	57.68 ± 3.14	-
	CUR-Cu	6.55 ± 0.17	193.20 ± 20.52*	3.3
	CUR-Mg	6.72 ± 0.14	76.64 ± 9.91	1.3
	CUR-Fe	6.56 ± 0.10	149.49 ± 11.33*	2.6
SMEDDS (1:8:1)	CUR	6.78 ± 0.19	57.46 ± 4.09	-
	CUR-Cu	6.78 ± 0.19	197.30 ± 15.06*	3.4
	CUR-Mg	6.73 ± 0.24	84.81 ± 7.97	1.5
	CUR-Fe	6.70 ± 0.16	177.78 ± 5.87*	3.1

Note: * indicates statistically significant difference at $p < 0.05$ between CUR and CUR metallocomplexes.

Solubility of CUR and CUR metallocomplexes in water and SMEDDSs

As shown in Figure 7, CUR and its metallocomplexes are practically insoluble in water (<1 µg/mL) but they were ~287-986-folds more soluble in both SMEDDSs. The solubility of CUR

and its metallocomplexes in both SMEDDSs (1:7:2 and 1:8:1) decreased in the order of CUR-Cu > CUR-Fe > CUR-Mg > CUR. The solubility of CUR-Cu, CUR-Mg and CUR-Fe in both SMEDDSs were 3.4-, 2.8- and 1.4-times, respectively; higher than that of CUR in both SMEDDSs.

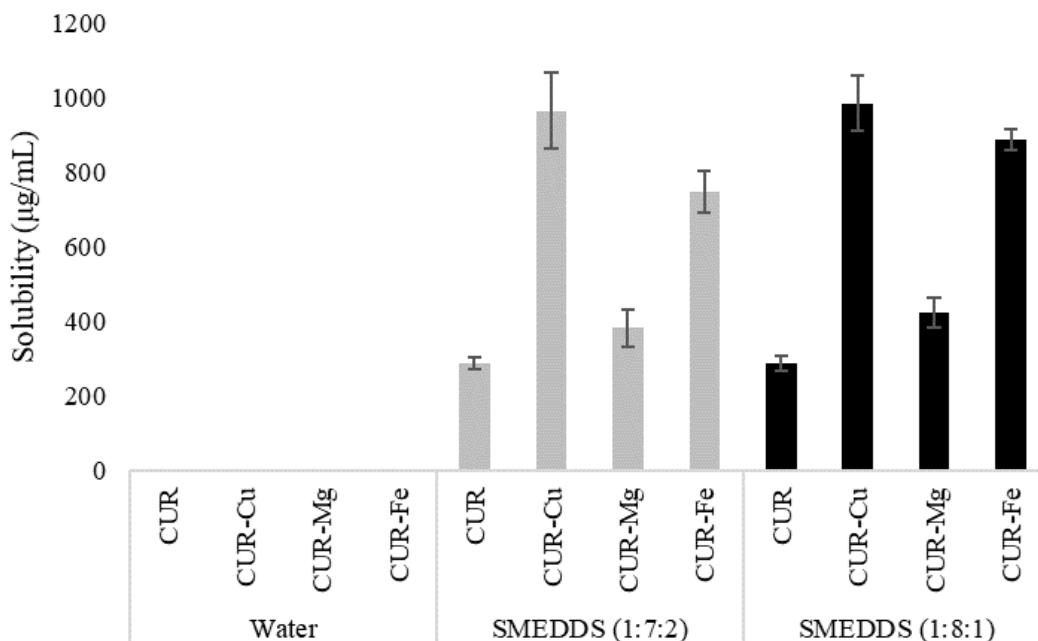


Figure 7. Solubility of CUR and CUR metallocomplexes in water and SMEDDSs (1:7:2 and 1:8:1).

Antioxidative activity of CUR and CUR metallocomplexes in SMEDDSs

The antioxidative potential of CUR and CUR metallocomplexes is evaluated by DPPH assay to determine their potential to scavenge free radicals. When free radical DPPH receives a hydrogen atom from an antioxidant, it is reduced to a hydrazine, leading to a drop in the absorbance of the reaction along with discolouration of violet to yellow⁽³⁵⁾. The antioxidative activity of non-SMEDDS samples (1mg/mL) decreased in the order of CUR \approx CUR-Mg > CUR-Cu > CUR-Fe. The antioxidative activity of CUR metallocomplexes (μ g/mL) in 1:7:2 SMEDDSs decreased in the order of: CUR-Cu > CUR-Mg > CUR > CUR-Fe. Meanwhile, the antioxidative activity for CUR metallocomplexes in 1:8:1 SMEDDSs decreased in the order of: CUR-Cu > CUR-Mg \approx CUR > CUR-Fe (Table 5). In both formulations, CUR-Cu SMEDDSs displayed ~2-

folds higher %RSA compared to CUR SMEDDSs, meanwhile; CUR-Mg and CUR displayed comparable %RSA. In both formulations or non-SMEDDS, CUR-Fe displayed the lowest %RSA (~6-7%) and this could be attributed to its instability in the 1:1 metal-ligand stoichiometry. The coordination bond distance between a metal and a ligand increases with increasing number of unpaired electrons⁽³⁶⁾. The Fe³⁺ ion has five unpaired electrons, giving rise to its high oxidizing properties. Fe³⁺ must stabilize itself by attracting more electrons, thus, using a metal-to-ligand stoichiometry of 1:3 might render Fe³⁺ less reactive and form a stable complex with CUR⁽³⁷⁾. There are no significant differences ($p > 0.05$) were found in the %RSA between both formulations (1:7:2 and 1:8:1) of SMEDDSs, therefore, the %RSA is not influenced by the concentrations of surfactant and co-surfactant.

Table 5. %RSA of CUR and CUR metallocomplexes

Samples		%RSA
Non-SMEDDS	CUR	53.41 \pm 2.21
	CUR-Cu	41.95 \pm 2.00
	CUR-Mg	50.28 \pm 3.47
	CUR-Fe	20.41 \pm 3.24
SMEDDS (1:7:2)	CUR	9.60 \pm 1.20
	CUR-Cu	24.70 \pm 2.69*
	CUR-Mg	12.37 \pm 1.95
	CUR-Fe	7.17 \pm 0.42
SMEDDS (1:8:1)	CUR	11.31 \pm 0.58
	CUR-Cu	22.68 \pm 2.25*
	CUR-Mg	11.21 \pm 2.30
	CUR-Fe	6.52 \pm 0.89

Note: * indicates statistically significant difference at $p < 0.05$ between CUR and CUR metallocomplexes.

Conclusion

In summary, CUR metallocomplexes (CUR-Cu, CUR-Mg and CUR-Fe) were synthesized and characterized by FTIR and UV-vis spectroscopies. The SMEDDSs consisting of varying amounts of palm oil (oily phase), Tween 80 (surfactant) and PEG 400 (co-surfactant) (1:7:2 and 1:8:1) were used to encapsulate CUR and CUR metallocomplexes. All of the SMEDDSs were monophasic, clear and neutral in pH (6.55 - 6.78). CUR-Cu exhibited the highest solubility in both SMEDDSs which were ~3-folds higher than CUR in SMEDDSs. The antioxidative activity decreases in the manner of: CUR-Cu > CUR, CUR-Mg > CUR-Fe in both SMEDDSs formulations. This research indicates that the SMEDDS could be a promising approach for delivering CUR metallocomplexes.

Acknowledgment

We thank Ms. Chia Lee Huang for her valuable comments on the work.

Conflicts of Interest

We hereby declare that there is no conflict of interest.

Funding

This research is supported by SEGi University, Final Year Project Fund.

Ethics Statements

No human subjects nor living animals were used in this study, thus, no consents were required.

Author Contribution

Wei Sean Mah: Final Year BPharm student; Shu Xian Chong: Supervisor.

References

1. Sun YM, Zhang HY and Chen DZ, et al. Theoretical elucidation on the antioxidant mechanism of curcumin: A DFT study, *Org Lett*. 2002; 4 (17): 2909–2911.
2. Prasad D, Praveen A and Mahapatra S, et al. Existence of β -diketone form of curcuminoids revealed by NMR spectroscopy, *Food Chem*. 2021; 360: 130000.
3. Urošević M, Nikolić L and Gajić I. et al. Curcumin: Biological activities and modern pharmaceutical forms. *antibiotics* (Basel). 2022; 11(2):135.
4. Prasad S, DuBourdieu D and Srivastava A, et al. Metal-curcumin complexes in therapeutics: an approach to enhance pharmacological effects of curcumin. *Int J Mol Sci*. 2021; 22(13):7094.
5. Thakam A and Saewan N. Antioxidant activities of curcumin-metal complexes. *Thai J Agric Sci*. 2011; 44: 188–193.
6. Arenaza-Corona, A, Obregón-Mendoza MA and Meza-Morales W, et al. The homoleptic curcumin-copper single crystal (ML2): A long awaited breakthrough in the field of curcumin metal complexes. *Mol*. 2023; 28 (16): 6033.
7. Mohammadi K, Thompson KH and Patrick BO, et al. Synthesis and characterization of dual function vanadyl, gallium and indium curcumin complexes for medicinal applications. *J Inorg Biochem*. 2005; 99 (11): 2217–2225.
8. Silberstein S, Spierings EL and Kunkel T. Celecoxib oral solution and the benefits of self-microemulsifying drug delivery systems (SMEDDS) technology: A narrative review. *Pain Ther*. 2023;12 (5): 1109–1119.
9. Kang BK, Lee JS and Chon SK, et al. Development of self-microemulsifying drug delivery systems (SMEDDS) for oral bioavailability enhancement of simvastatin in beagle dogs. *Int. J Pharm*. 2004; 274 (1–2): 65–73.
10. Liu CS, Chen L and Hu YN, et al. Self-microemulsifying drug delivery system for improved oral delivery and hypnotic efficacy of ferulic acid. *Int J Nanomedicine* 2020; 15: 2059–2070.
11. Kawakami K, Yoshikawa T, and Hayashi T, et al. Microemulsion formulation for enhanced absorption of poorly soluble drugs: II. in vivo study. *J Controlled Release*. 2002; 81 (1): 75–82.
12. Chhitij T, Seo JE and Keum T, et al. Optimized self-microemulsifying drug delivery system improves the oral bioavailability and brain delivery of coenzyme Q10. *Drug Deliv*. 2022; 29 (1): 2330–2342.
13. Xia F, Chen Z and Zhu Q, et al. Gastrointestinal lipolysis and trans-epithelial transport of SMEDDS via oral route. *Acta Pharm Sin B*. 2021; 11 (4): 1010–1020.
14. Dokania S and Joshi AK. Self-microemulsifying drug delivery system (SMEDDS)--Challenges and road ahead. *Drug Deliv*. 2015; 22 (6): 675–690.
15. Sareen R, Jain N and Dhar KL. Curcumin-Zn(II) complex for enhanced solubility and stability: An approach for improved delivery and pharmacodynamic effects. *Pharm Dev Technol*. 2016; 21 (5): 630–635.
16. Muniandy G and Chong SX. Optimization of curcumin microemulsions using palm oil. *Malays J Pharm Sci*. 2022; 20 (2): 27–38.
17. Tang H, Xiang S and Li X, et al. Preparation and in vitro performance evaluation of resveratrol for oral self-microemulsion. *PLOS ONE*. 2019; 14 (4): e0214544.
18. Prasad S, DuBourdieu D and Srivastava A, et al. Metal curcumin complexes in therapeutics: An approach to enhance pharmacological effects of curcumin. *Int J Mol Sci*. 2021; 22 (13): 7094.
19. Lalman J and Bagley D. Extracting long-chain fatty acids from a fermentation medium. *J Amer Oil Chem Soc*. 2004; 81: 105–110.

20. Leung HM, Harada T and Kee TW. Delivery of curcumin and medicinal effects of the Copper(II)-curcumin complexes. *Curr Pharm Des.* 2013; 19 (11): 2070–2083.
21. Leung HM, Pham DT and Lincoln SF, et al. Femtosecond transient absorption spectroscopy of Copper(II)-Curcumin complexes. *Phys Chem Chem Phys.* 2012; 14 (39): 13580.
22. Peni P, Sasri R and Silalahi I. Synthesis of metal–curcumin complex compounds (M = Na⁺, Mg²⁺, Cu²⁺). *Jurnal Kimia Sains Dan Aplikasi.* 2020; 23: 75–82.
23. Hieu TQ and Thao DT. Enhancing the solubility of curcumin metal complexes and investigating some of their biological activities. *J Chem.* 2019; 2019: e8082195.
24. Altundağ EM, Özbilenler C and Ustürk S, et al. Metal-based curcumin and quercetin complexes: Cell viability, ROS production and antioxidant activity. *J Mol Struct.* 2021; 1245: 131107.
25. Del Prado-Audelo ML, Caballero-Florán IH and Meza-Toledo JA, et al. Formulations of curcumin nanoparticles for brain diseases. *Biomol.* 2019; 9 (2): 56.
26. Payton F, Sandusky P and Alworth WL. NMR study of the solution structure of curcumin. *J Nat Prod.* 2007; 70 (2): 143–146.
27. Barik A, Mishra B and Shen L, et al. Evaluation of a new Copper(II)-curcumin complex as superoxide dismutase mimic and its free radical reactions. *Free Radic Bio Med.* 2005; 39 (6): 811–822.
28. Gurram AK, Deshpande PB and Kar SS., et al. Role of components in the formation of self-microemulsifying drug delivery systems. *Indian J Pharm Sci.* 2015; 77 (3): 249–257.
29. Shah A, Thool P and Sorathiya K., et al. Effect of different polysorbates on development of self-microemulsifying drug delivery systems using medium chain lipids. *Drug Deve Ind Pharm.* 2018; 44 (2): 215–223.
30. Akula S, Gurram AK and Devireddy SR. Self-microemulsifying drug delivery systems: An attractive strategy for enhanced therapeutic profile. *Int Sch Res Notices.* 2014;2014: e964051.
31. Timur SS, Yöyen-Ermiş D and Esendağlı G, et al. Efficacy of a novel LyP-1-containing self-microemulsifying drug delivery system (SMEDDS) for active targeting to breast cancer. *Eur J Pharm Biopharm.* 2019; 136: 138–146.
32. Patel MH and Sawant KK. Self microemulsifying drug delivery system of lurasidone hydrochloride for enhanced oral bioavailability by lymphatic targeting: In vitro, Caco-2 cell line and in vivo evaluation. *Eur J Pharm Sci.* 2019; 138, 105027.
33. Zebib B, Mouloungui Z and Noirot V. Stabilization of curcumin by complexation with divalent cations in glycerol/water system. *Bioinorg Chem Appl.* 2010; 2010: e292760.
34. Thakkar V and Shah A. Optimization of self micro emulsifying drug delivery system containing curcumin and artemisinin using D-optimal mixture design. *Saudi Journal of Medical and Pharmaceutical Sciences.* 2017; 3, 388–398.
35. Baliyan S, Mukherjee R and Priyadarshini A, et al. Determination of antioxidants by DPPH radical scavenging activity and quantitative phytochemical analysis of *Ficus Religiosa*. *Mol.* 2022; 27 (4): 1326.
36. Pranata A and Surya R. Effects of the addition of complexing agents on curcumin stability using accelerated shelf life testing. *J Phys Conf Ser.* 2021; 2049 (1): 012034.
37. Khalil MI, Al-Zahem AM and Al-Qunaibit MH. Synthesis, characterization, Mössbauer parameters, and antitumor activity of Fe(III) curcumin complex. *Bioinorg Chem Appl.* 2013; 2013: e982423.